Improving performance of 750-Mb/s visible light communication system using adaptive Nyquist windowing

Rongling Li (李荣玲), Yuanquan Wang (王源泉), Chanjuan Tang (汤婵娟), Yiguang Wang (王一光), Huiliang Shang (商慧亮), and Nan Chi (迟 楠)*

Department of Communication Science and Engineering, Fudan University, Shanghai 200433, China

**Corresponding author: nanchi@fudan.edu.cn*

Received March 7, 2013; accepted May 13, 2013; posted online August 2, 2013

We propose a configuration of a wavelength division multiplexing (WDM)-visible light communication (VLC) system using orthogonal frequency division multiplexing (OFDM) modulation and an adaptive Nyquist windowing of the OFDM signal in the receiver. Based on this configuration, we demonstrate a 750-Mb/s WDM-VLC transmission based on RGB light-emitting diode (LED) with a distance of 70 cm. The measured bit error rate (BER) for all channels are under the pre-forward error correction limit of 3.8×10^{-3}. The BER performances of all the channels of the proposed WDM-VLC system show considerable improvement compared with those of the system without Nyquist windowing.

OCIS codes: 060.2605, 140.7300, 070.2025.

doi: 10.3788/COL201311.080605.

The use of light-emitting diodes (LEDs) as replacement for fluorescent and incandescent lamps for lighting has become an obvious trend[1]. As the most promising device for next-generation illumination, LED has several advantages, including high efficiency, long life, low cost, low power consumption, and security[2]. The use of LEDs for both illumination and communication has made visible light communication (VLC) a hot research topic in recent years[1−14]. VLC is a type of optical wireless technology in which signals are modulated onto the light emitted by LEDs for transmission. VLC has no electromagnetic spectrum regulation and does not pose a potential threat to humans.

The main challenge in the development of VLC is the bandwidth of white LEDs (phosphor-based and RGB LEDs). RGB LEDs are very promising in high-speed transmission because of their wide bandwidth[15]. Researchers have adopted spectrally efficient modulation techniques such as orthogonal frequency division multiplexing (OFDM) or discrete multitone(DMT) in VLC systems to fully utilize the bandwidth of RGB LEDs[5−11]. A demonstration of 3.4 -Gb/s wavelength division multiplexing(WDM)-VLC link based on RGB LED using DMT modulation has been reported[11]. The system transmitted within 10 cm and used an avalanche photodiode (PD) as receiver. The WDM-VLC system demonstrated in the current study transmits 70 cm at a bit rate of 750 Mb/s and uses a low-cost PIN (PD)with a bit error rate (BER) performance similar to that in Ref. [11]. The measured BER performances for all channels are under the pre-forward error correction (FEC) limit of 3.8×10^{-3}[16].

The OFDM signal is very sensitive to frequency offset in the receiver. In the OFDM system, the frequency offset will break the orthogonality between the subcarriers, thereby leading to intercarrier interference (ICI). In this letter, we use an adaptive Nyquist window in the receiver to reduce the impact of frequency offset. Despite the use of a Nyquist windowing, the complexity of signal processing does not increase[15]. The experiment results show an improvement in BER performance by up to 4 dB (blue) after using an adaptive Nyquist windowing.

The configuration of the proposed WDM-VLC system using an adaptive Nyquist windowing is presented in Fig. 1. In this scheme, quadrature amplitude modulation (QAM) and OFDM modulation were employed to increase the data rate. An adaptive Nyquist windowing was employed to improve the OFDM signal reception. Equalization in the frequency domain is necessary because the channel response is unbalanced. Pre-and post-equalizations were designed and applied by software based on channel knowledge to compensate for the poor channel response of the LED.

RGB LED (Cree Xlamp MC-E) was used as a transmitter. This kind of RGB LED consists of four chips radiating red (625 nm), green (530 nm), blue (455 nm), and white light, respectively. It generates a luminous flux of about 106 lm at 350 mA bias currents. The red, green, and blue channels of the RGB LED were used to carry independent signals.

At the transmitter, a stream of random binary data was modulated using 32QAM formats and then passed to an OFDM encoder. Here, 64 OFDM subcarriers were used, and a cyclic prefix(CP) was also inserted. The output complex signal was filtered using low-pass filters (LPFs) and converted into analog signal in the D/A convertors. The electrical 32QAM OFDM signal was modulated onto the radio frequency (RF) carrier at 31.25 MHz. Given the noisy channel from direct current (DC) to 5 MHz, the signal frequency band from 6.25 to 56.25 MHz was chosen instead of the baseband. The output signal and DC-bias voltage were combined through a Bias Tee and applied to the red/green/blue chip of the RGB LED serving as a transmitter. One channel was studied at a time. For each channel, the bit rate was 250 Mb/s, and the total speed was 750 Mb/s. The LED 3 -dB bandwidth was about 6 MHz for all three channels, and the modulation depth was 1.

At the receiver, the optical signal was focused on the PD (Hamamatsu S6968, 50 MHz bandwidth) through a lens (100 mm focus length, 75 mm diameter)

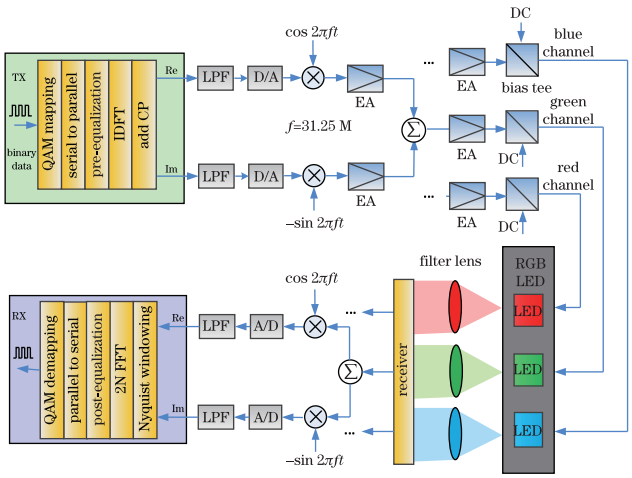

Fig. 1. Configuration of the WDM-VLC system using a Nyquist windowing. EA: electronic amplifier.

and converted into an electrical signal. After down-converting to the baseband, the electrical signal was then converted to a digital signal in the A/D convertor. Further off-line signal processing, which is the inverse of the QAM-OFDM encoder, is shown in Fig. 1.

In general, the CP of the digital QAM-OFDM signal is first removed to recover the carrier orthogonality. Then, a discrete Fourier transform (DFT) of the remaining N samples, which is defined as

$$X(n) = \sum_{k=0}^{N-1} x(k) \mathrm{e}^{-\mathrm{j}kn\frac{2\pi}{N}}, \tag{1}$$

where $x(k)$ is a sampled signal containing N individual subcarriers and is given by

$$x(k) = \sum_{i=1}^{N} A_i \mathrm{e}^{\mathrm{j}2\pi f_i k}, \tag{2}$$

where A_i is the data carried by the i_{th} subcarrier, and f_i is the normalized frequency of the i_{th} subcarrier. Hence, the DFT of the sampled signal can be expressed as

$$\begin{aligned} X(n) &= \sum_{k=0}^{N-1} \sum_{i=1}^{N} A_i \mathrm{e}^{\mathrm{j}2\pi k(f_i - \frac{n}{N})} \\ &= \sum_{i=1}^{N} A_i \mathrm{e}^{\mathrm{j}\pi(f_i N - n)\frac{N-1}{N}} \frac{\sin\left[\pi\left(f_i N - n\right)\right]}{\sin\left[\pi\left(f_i N - n\right)/N\right]}. \end{aligned} \tag{3}$$

For the i_{th} subcarrier, the amplitude of $X(n)$ is similar to a sinc function (Fig. 2). When f_i is equal to the normalized frequency n/N, the data carried by the i_{th} subcarrier are extracted, and the amplitude at other subcarriers are equal to zero. Thus, the DFT process acts as a set of filters with different center frequencies (Fig. 2).

In an ideal case, the DFT performs carrier filtering and allows the separation of the carriers without ICI. However, the frequency offset of the system will produce DFT leakage. In case of leakage, the output of a DFT filter consists of all subcarriers. Thus, the subcarriers of the OFDM signal will perceive and interfere with one another, thereby leading to ICI. In the proposed VLC system, the frequency offset occurred during the signal down-conversion process at the receiver side and the mismatch of the sampling clock between the transmitter and receiver. As the OFDM signal was modulated on a subcarrier of 31.25 MHz for transmission, the frequency difference between the carrier signal and the local RF source would produce a frequency offset. In addition, the mismatch of the sampling clocks, which often occurs because of the instability of the crystal oscillator, would cause frequency offset as frequency increases. This kind of frequency offset is discussed in detail in Ref. [17].

As shown in Fig. 2, the ICI results from the side lobes of the DFT filters. The use of a Nyquist window can reduce the side lobes and conserve carrier orthogonality simultaneously. By using Nyquist windowing in the time domain, the frequency response of the DFT filter can be improved, and the influence of leakage can be reduced.

The manner by which an adaptive Nyquist windowing is implemented is described in the following paragraphs[15]. The length of CP is T_v, including V samples. The OFDM symbol period is T_u consisting of N samples. The $N+V$ samples are symmetrically windowed by a Nyquist window. In the experiments, N was 64, and V was 8. The window function $w(\mathrm{t})$ is defined as

$$w(t) = \begin{cases} 0 \le |t| \le \frac{(1-\alpha)T_u}{2} \\ \frac{1}{2}\left[1 - \sin\frac{\pi(|t|-T_u/2)}{\alpha T_u}\right] \frac{(1-\alpha)T_u}{2} \le |t| \le \frac{(1+\alpha)T_u}{2} \\ 0 \, |t| \ge \frac{(1+\alpha)T_u}{2} \end{cases}. \tag{4}$$

The selection of a roll-off factor α depends on experience and on the length of CP. We chose the value of α according to the experiment results . In practice, the α value may be between 0 and 0.3.

After Nyquist windowing, a symmetrical zero padding is performed to complete a total of $2N$ samples. Then a FFT can be used to calculate the $2N$ coefficients a_k. Only odd or even coefficients containing the carriers are used to extract information; the other "ghost coefficients" containing only disturbances such as carrier

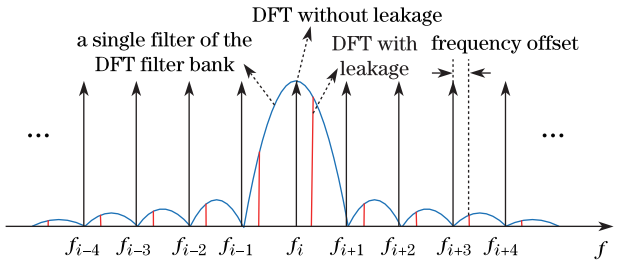

Fig. 2. DFT filter bank consisting of N filters.

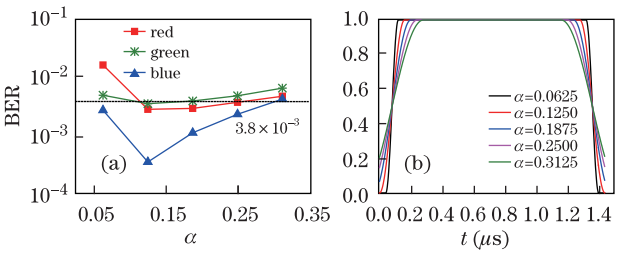

Fig. 3. (a) BER versus roll-off factor α. (b) Nyquist window function depending on roll-off factor α.

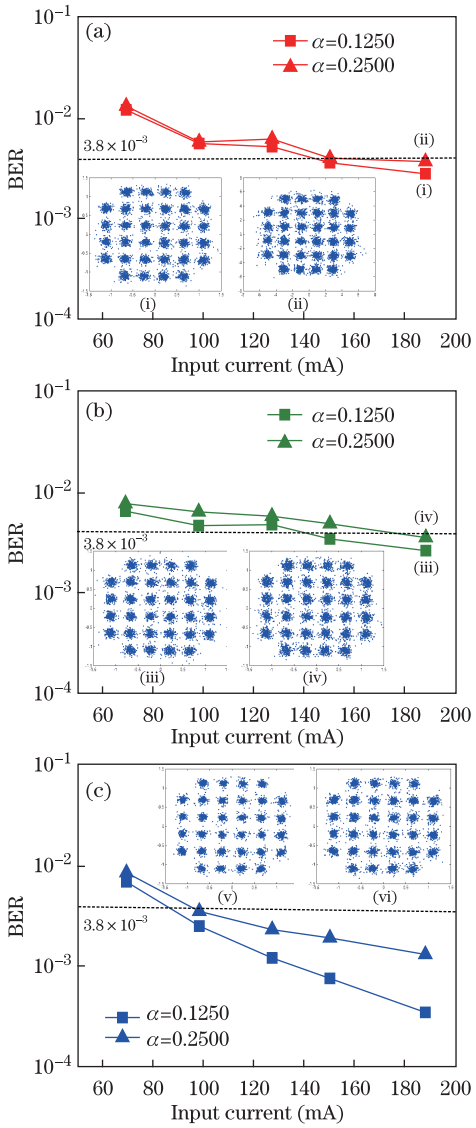

Fig. 4. BER versus input current when $\alpha = 0.1250$ and $\alpha = 0.2500$ for (a) red, (b) green, and (c) blue channels.

leakage are discarded. By avoiding the computation of ghost coefficients, the complexity of the $2N$-FFT can be reduced near to that of the N-FFT.

Using our configuration, we demonstrate a 750 -Mb/s transmission of the proposed system. At the transmitter, arbitary waveform generator (AWG) (Tektronix AWG 7122C) is used to generate QAM-OFDM signals. Up-sampling by a factor of 10 is employed, and the sampling rate of AWG is 500 MS/s. At the receiver, data are recorded by a commercial high-speed digital oscilloscope (Tektronix TDS 6604) with a sampling rate of 500 MS/s. The maximum bias current for the RGB LED is set to 188 mA.

As mentioned previously, the selection of α value can affect system performance. Thus, the ways in which BER performances change with α are first investigated, as shown in Fig. 3(a). The input current is set to 188 mA. The optimum α is found to be 0.125 for all three channels. The side lobes become lower with the increase of α, but the useful signal (OFDM symbol) attenuates at the same time. Thus, an optimum α should be selected. In our experiments, the optimum α equals T_v/T_u, that is, 0.125. The BER versus α curves of the three channels differ because of different channel responses. The BER performance of the blue channel is better than that of the other two channels because of its superior channel response. Figure 3(b) presents the Nyquist window function $w(t)$ depending on the roll-off factor α.

To deepen our understanding of the effect of the α value, we compare the BER performance versus the input current when α is set to the optimum value of 0.125 and to the suboptimum value of 0.25. The results are given in Fig. 4. The inserted Figs. i to vi are the constellations for the three channels when the input current is 188 mA. Increase in the current results in the improvement of BER performances for the red, green, and blue channels. The input current cannot be too large that it exceeds the linear region of the LED. Obvious differences exist between the BER performances of $\alpha = 0.125$ and $\alpha = 0.25$.

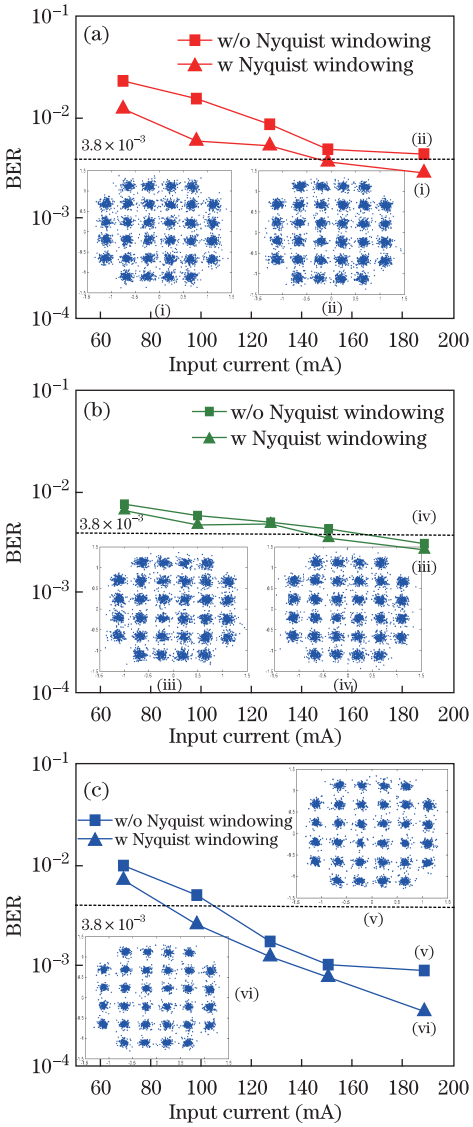

Fig. 5. BER versus input current with and without Nyquist windowing for (a) red, (b) green, and (c) blue channels.

The differences increase when the input current increases. When the input current is set to 188 mA, the BER performances are 2.8×10^{-3} (red), 2.6×10^{-3}

(green), and 3.4375×10^{-4} (blue) for $\alpha = 0.125$; 3.7×10^{-3} (red), 3.5×10^{-3} (green), and 1.3×10^{-3} (blue) for $\alpha = 0.25$. In other words, the performance of the system with $\alpha = 0.125$ is better than that with $\alpha = 0.25$.

The BER performances of the system with and without an adaptive windowing are measured to clearly show the impact of an adaptive Nyquist windowing. The roll-off factor α is set to 0.125. As shown in Fig. 5, the BER performance of the system exhibits obvious improvement for the red and blue channels after the adoption of an adaptive Nyquist windowing. The BER improvement for the green channel is very small, probably because of its channel response being the worst among those of the other channels. Figure 5 also shows the constellations for the three channels when the input current is 188 mA. Given this input current, the BER performances are 2.8×10^{-3} (red), 2.6×10^{-3} (green), and 3.4375×10^{-4} (blue), respectively. The BER performances of the system without Nyquist windowing are 4.3×10^{-3} (red), 3×10^{-3} (green), and 8.75×10^{-4} (blue), respectively.

In conclusion, we propose a novel configuration of the WDM-VLC system that adopts QAM-OFDM modulation and an adaptive Nyquist windowing. Based on this configuration, we successfully demonstrate a 750 -Mb/s WDM-VLC transmission experiment using RGB LED. In the experiment, signals are modulated onto three optical wavelengths (red, green, and blue). The transmission distance can be as long as 70 cm. The measured BER for all channels are under the pre-FEC limit of 3.8×10^{-3} after 70 -cm free-space transmission. The complexity of the signal processing does not increase despite the use of a Nyquist windowing. The BER performances of the proposed WDM-VLC system show considerable improvement compared with those of the system without Nyquist windowing. The results show that Nyquist windowing is useful for improving the performance of WDM-VLC systems.

This work was supported by the National "973" Program of China (No. 2010CB328300), the National Natural Science Foundation of China (Nos. 61107064 and 61177071), the National "863" Program of China (Nos. 2011AA010302 and 2012AA011302), the National Key Technology R&D Program (No. 2012BAH18B00), and the Key Program of Shanghai Science and Technology Association (No. 12dz1143000).

References

1. A. B. Siddique and M. Tahir, in *Proceedings of CCNC 2011* 1026 (2011).
2. K.-D. Langer, J. Vučić C. Kottke, L. F. del Rosal, S. Nerreter, and J. Walewsk, in *Proceedings of ICTON 2009* Mo.B5.3 (2009).
3. H. Le Minh, D. O'Brien, G. Faulkner, L. Zeng, K. Lee, D. Jung, and Y. Oh, IEEE Photon. Technol. Lett. **20,** 1243 (2008).
4. H. Le Minh, D. O'Brien, G. Faulkner, L. Zeng, K. Lee, D. Jung, and Y. Oh, in *Proceedings of ECOC 2008* P.6.09 (2008)
5. J. Vučić C. Kottke, S. Nerreter, K.-D. Langer, and J. W. Walewski, J. Lightwave Technol. **28,** 3512 (2010).
6. C. Kottke, K. Habel, L. Grobe, J. Hilt, L. F. del Rosal, A. Paraskevopoulos, and K.-D. Langer, in *Proceedings of ICTON 2012* We.B4.1 (2012).
7. J. Vučić C. Kottke, K. Habel, and K.-D. Langer, in *Proceedings of OFC/NFOEC 2011* OWB6 (2011).
8. A. M. Khalid, G. Cossu, R. Corsini, P. Choudhury, and E. Ciaramella, IEEE Photon. J. **4,** 1465 (2012)
9. J. Vučić C. Kottke, S. Nerreter, A. Büttner, K.-D. Langer, and J. W. Walewski, IEEE Photon. Technol. Lett. **21,** 1511 (2009).
10. Y. Wang, Y. Wang, N. Chi, J. Yu, and H. Shang, Opt. Express **21,** 1203 (2013).
11. G. Cossu, A. M. Khalid, P. Choudhury, R. Corsini, and E. Ciaramella, Opt. Express **20,** B501 (2012).
12. Y. Wu, A. Yang, L. Feng, and Y. Sun, Chin. Opt. Lett. **11,** 030601 (2013).
13. Z. Huang and Y. Ji, Chin. Opt. Lett. **10,** 050602 (2012).
14. Y. Zheng and M. Zhang, in *Proceedings of SOPO 2010* 1 (2010).
15. C. Muschallik, IEEE Trans. Consum. Electron. **42,** 259 (1996).
16. R. Elschner, T. Richter, T. Kato, S. Watanabe, and C. Schubert, in *Proceedings of OFC 2012* PDP5C.8 (2012).
17. L. Tao, J. Yu, J. Zhang, Y. Shao, and N. Chi, Photon. Technol. Lett. **25,** 851 (2013).